J Neurosurg 119:1176–1193, 2013

Foramen ovale puncture, lesioning accuracy, and avoiding complications: microsurgical anatomy study with clinical implications

Laboratory investigation

Maria Peris-Celda, M.D., Ph.D.,[1,2] Francesca Graziano, M.D.,[1] Vittorio Russo, M.D.,[1] Robert A. Mericle, M.D.,[3] and Arthur J. Ulm, M.D.[1]

[1]Microsurgical Neuroanatomy Laboratory, Department of Neurosurgery, Louisiana State University Health Sciences Center, New Orleans, Louisiana; [2]Department of Neurosurgery, La Fe University Hospital, Valencia, Spain; and [3]Department of Neurosurgery, Vanderbilt University Medical Center, Nashville, Tennessee

Object. Foramen ovale (FO) puncture allows for trigeminal neuralgia treatment, FO electrode placement, and selected biopsy studies. The goals of this study were to demonstrate the anatomical basis of complications related to FO puncture, and provide anatomical landmarks for improvement of safety, selective lesioning of the trigeminal nerve (TN), and optimal placement of electrodes.

Methods. Both sides of 50 dry skulls were studied to obtain the distances from the FO to relevant cranial base references. A total of 36 sides from 18 formalin-fixed specimens were dissected for Meckel cave and TN measurements. The best radiographic projection for FO visualization was assessed in 40 skulls, and the optimal trajectory angles, insertion depths, and topographies of the lesions were evaluated in 17 specimens. In addition, the differences in postoperative pain relief after the radiofrequency procedure among different branches of the TN were statistically assessed in 49 patients to determine if there was any TN branch less efficiently targeted.

Results. Most severe complications during FO puncture are related to incorrect needle placement intracranially or extracranially. The needle should be inserted 25 mm lateral to the oral commissure, forming an approximately 45° angle with the hard palate in the lateral radiographic view, directed 20° medially in the anteroposterior view. Once the needle reaches the FO, it can be advanced by 20 mm, on average, up to the petrous ridge. If the needle/radiofrequency electrode tip remains more than 18 mm away from the midline, injury to the cavernous carotid artery is minimized. Anatomically there is less potential for complications when the needle/radiofrequency electrode is advanced no more than 2 mm away from the clival line in the lateral view, when the needle pierces the medial part of the FO toward the medial part of the trigeminal impression in the petrous ridge, and no more than 4 mm in the lateral part. The 40°/45° inferior transfacial–20° oblique radiographic projection visualized 96.2% of the FOs in dry skulls, and the remainder were not visualized in any other projection of the radiograph. Patients with V1 involvement experienced postoperative pain more frequently than did patients with V2 or V3 involvement. Anatomical targeting of V1 in specimens was more efficiently achieved by inserting the needle in the medial third of the FO; for V2 targeting, in the middle of the FO; and for V3 targeting, in the lateral third of the FO.

Conclusions. Knowledge of the extracranial and intracranial anatomical relationships of the FO is essential to understanding and avoiding complications during FO puncture. These data suggest that better radiographic visualization of the FO can improve lesioning accuracy depending on the part of the FO to be punctured. The angles and safety distances obtained may help the neurosurgeon minimize complications during FO puncture and TN lesioning. *(http://thejns.org/doi/abs/10.3171/2013.1.JNS12743)*

Key Words • **foramen ovale** • **puncture** • **microsurgical anatomy** • **radiofrequency** • **trigeminal nerve** • **pain**

Foramen ovale puncture was first described by Härtel in 1914[18] as a percutaneous route to the Meckel cave to treat trigeminal neuralgia. Microvascular decompression induces little or no hypesthesia and is usually the treatment of choice for young patients without comorbidities.[3] However, less invasive techniques, including FO puncture, are preferred in older patients and have resulted in significant and persistent pain relief. Foramen

Abbreviations used in this paper: AP = anteroposterior; FO = foramen ovale; TN = trigeminal nerve.

This article contains some figures that are displayed in color online but in black-and-white in the print edition.

ovale puncture is followed by destruction of TN fibers using radiofrequency ablation, microcompression with a Fogarty catheter, or neurotoxic substances (glycerol). In functional neurosurgery, FO electrodes are placed percutaneously to register mesial temporal activity in patients with epilepsy[40,50,51,53] and some cases of biopsy sampling have been also reported.[2,4,28]

Although the FO puncture technique has been thoroughly reported with some variations, to our knowledge there are no detailed anatomical reports on this topic that explain the anatomical basis and safety distances to avoid major complications. Several articles have focused on improving the selectivity of the lesion based on functional data from clinical experience.[43,45,46] Complementary to this knowledge, anatomical research provides direct measurements and visualization as tools to improve the accuracy and selectivity of the lesions. The FO visualization rate with radiography and optimal angles of view remain within a wide range as reported in the literature,[9,11,12,14] and are mostly subject to the experience of the neurosurgeon.

The objectives of this article are to anatomically explain complications arising during FO puncture and how to avoid them, and to provide reliable anatomical landmarks to improve FO visualization and puncture technique, improve the effectiveness of selective lesioning of the TN, and determine optimal placement of FO electrodes.

Methods

Dry Skull Measurements

Fifty dry skull bases were studied from the exocranial surface to obtain measurements of the FO and distances to important osseous structures (Fig. 1, Table 1).

Dissection of Formalin-Fixed Specimens and Radiographic References

Eighteen formalin-fixed specimens were dissected for measurements of the Meckel cave (36 sides) and FO puncture trajectory (17 specimens, unilaterally). All the calvarias and brains were removed, as was the meningeal layer of the middle fossa dura mater covering the Meckel cave and cavernous sinus. The measurements performed are summarized in Table 2 and Fig. 2.

To study the ideal FO puncture trajectory, 2 lumbar puncture needles with stylets were inserted in each FO at

TABLE 1: Osseous relationships of the FO in the exocranial surface of the skull base*

Measurement	No. of Dry Skull Sides	Minimum	Maximum	Average	Standard Deviation
diameters (mm)					
A1	91	4.50	10.00	6.8187	1.12269
A2	91	2.50	5.20	3.6527	0.73248
B1	88	4.00	11.50	7.2420	1.47045
B2	88	2.50	10.00	5.5568	1.61785
C1	91	5.00	10.50	6.7451	1.15770
C2	91	3.00	8.00	5.2253	0.73509
D1	91	5.00	19.00	13.1593	2.45049
D2	91	4.50	16.00	8.0220	2.07133
distances (mm)					
1	71	7.50	17.00	11.4718	1.99622
2	90	0.50	6.00	2.8422	1.18568
3	91	12.00	30.00	19.2692	2.74399
4	91	8.00	17.50	12.1736	1.85471
5	89	3.50	13.00	6.7382	1.60783
6	77	0.00	10.00	2.3545	2.68169
7	90	0.00	8.00	0.8667	1.76864
μ	90	33.00	54.00	43.4056	4.73150
angles (°)					
α	77	23.00	48.00	39.3117	5.60606
β	85	0.00	10.00	1.1059	2.65484

* A1 and A2 = major and minor diameters of FO; B1 and B2 = major and minor diameters of foramen lacerum; C1 and C2 = major and minor diameters of carotid foramen; D1 and D2 = major and minor diameters of jugular foramen; 1 = distance from the FO to the mandibular fossa; 2 = distance from the FO to the foramen spinosum; 3 = distance from the FO to the jugular foramen; 4 = distance from the FO to the carotid foramen; 5 = distance from the FO to the foramen lacerum; 6 = distance from the base of the pterygoid processes to the FO; 7 = distance from μ to the FO. μ = distance from the external prominence above the second or third molar of the maxilla to the cranial base adjacent to the FO in a parallel to the midline; α = angle between a needle located over the external prominence above the second or third molar of the maxilla to the FO, and a line traced over the inferior part of the maxilla in the lateral view; β = angle between the needle and a parallel to the midline in an inferior view.

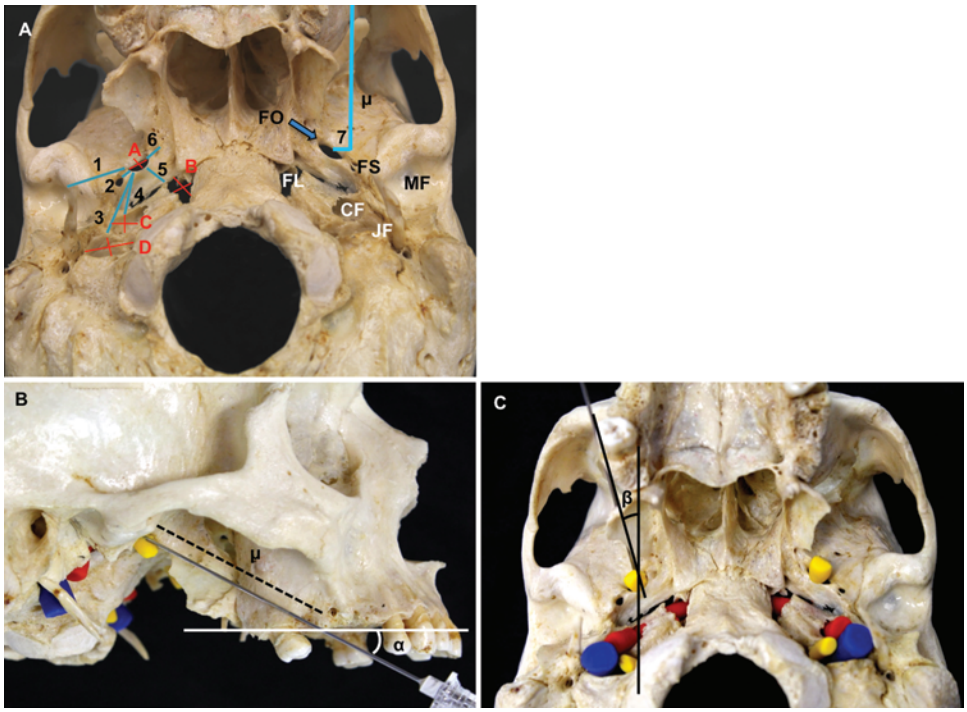

Fig. 1. Measurements of the osseous structures surrounding the FO from the exocranial surface of the skull base. **A:** Photograph of a dry skull with labels indicating diameters (A–D) and distances (1–7, μ). A = diameters of the FO; B = diameters of the foramen lacerum; C = diameters of the carotid foramen; D = diameters of the jugular foramen. 1 = distance from the FO to the mandibular fossa; 2 = distance from the FO to the foramen spinosum; 3 = distance from the FO to the jugular foramen; 4 = distance from the FO to the carotid foramen; 5 = distance from the FO to the foramen lacerum; 6 = distance from the base of the pterygoid processes to the foramen lacerum; 7 = distance from μ to the FO. μ = distance from the external prominence above the second or third molar of the maxilla to the cranial base adjacent to the FO in a line parallel to the midline; CF = carotid foramen; FL = foramen lacerum; FS = foramen spinosum; JF = jugular foramen; MF = mandibular fossa. **B and C:** Lateral (B) and inferior (C) views of the angle measurements performed on the dry skull bases: α = angle between a needle located over the external prominence above the second or third molar of the maxilla to the FO, and a line traced over the inferior part of the maxilla in the lateral view; β = angle between the needle and a line parallel to the midline in an inferior view. The V3 and pars nervosa of the jugular foramen are shown in *yellow*, carotid artery in *red*, and jugular vein in *blue* with molding material.

2 trajectories (lateral and medial; Fig. 3, Table 3). To accurately control the needle position, the needles were inserted from inside the skull base under direct visualization in the following manner. First, a needle forming the medial trajectory was inserted intracranially through the medial retrogasserian portion of the TN in the medial part of the trigeminal impression in the petrous ridge, and was directed to the medial part of the FO; its exit was medial to the mandible. Second, a needle forming the lateral trajectory was inserted intracranially through the lateral retrogasserian portion of the TN in the lateral part of the trigeminal impression in the petrous ridge, and was directed to the lateral part of the FO; its exit was also medial to the mandible.

After the initial insertion, the stylet was removed and reinserted extracranially from the face inside the previously inserted needle in a reverse manner. Then, the needle was removed. This procedure ensured that the stylet was located in the desired position in the medial and lateral trajectories. The tip end of both stylets was left in the petrous ridge border, so that one was located in the medial aspect of the trigeminal impression and the other in the lateral aspect.

A shorter additional needle was placed between the middle point of the FO and the posterior clinoid to estimate the angle of the Meckel cave in AP and lateral views. Anteroposterior and lateral radiographs were obtained in every specimen. The AP view was obtained with the radiography beam centered over the glabella, parallel to the orbitomeatal plane. This imaginary plane passes through the external acoustic meatus and the outer canthus of the eye. The lateral view, with superimposition of the superior orbital plates of the sphenoid bone and greater sphenoid wings, was obtained with the radiography beam directed perpendicular to a point 5 cm (2 inches) superior to the external acoustic meatus.

Radiographic Visualization of the FO

Forty dry skulls (79 sides) with mandibles were studied to obtain the best inferior transfacial/oblique projection to visualize the FO in both sides.

Clinical Review

It appears anatomically more difficult to access V1 in comparison with V2 and V3 during TN puncture; therefore, the objective of the clinical review was to determine if patients complaining of trigeminal neuralgia that involved V1 had less successful pain relief than patients with neuralgia involving V2 and V3. The outcomes of 57

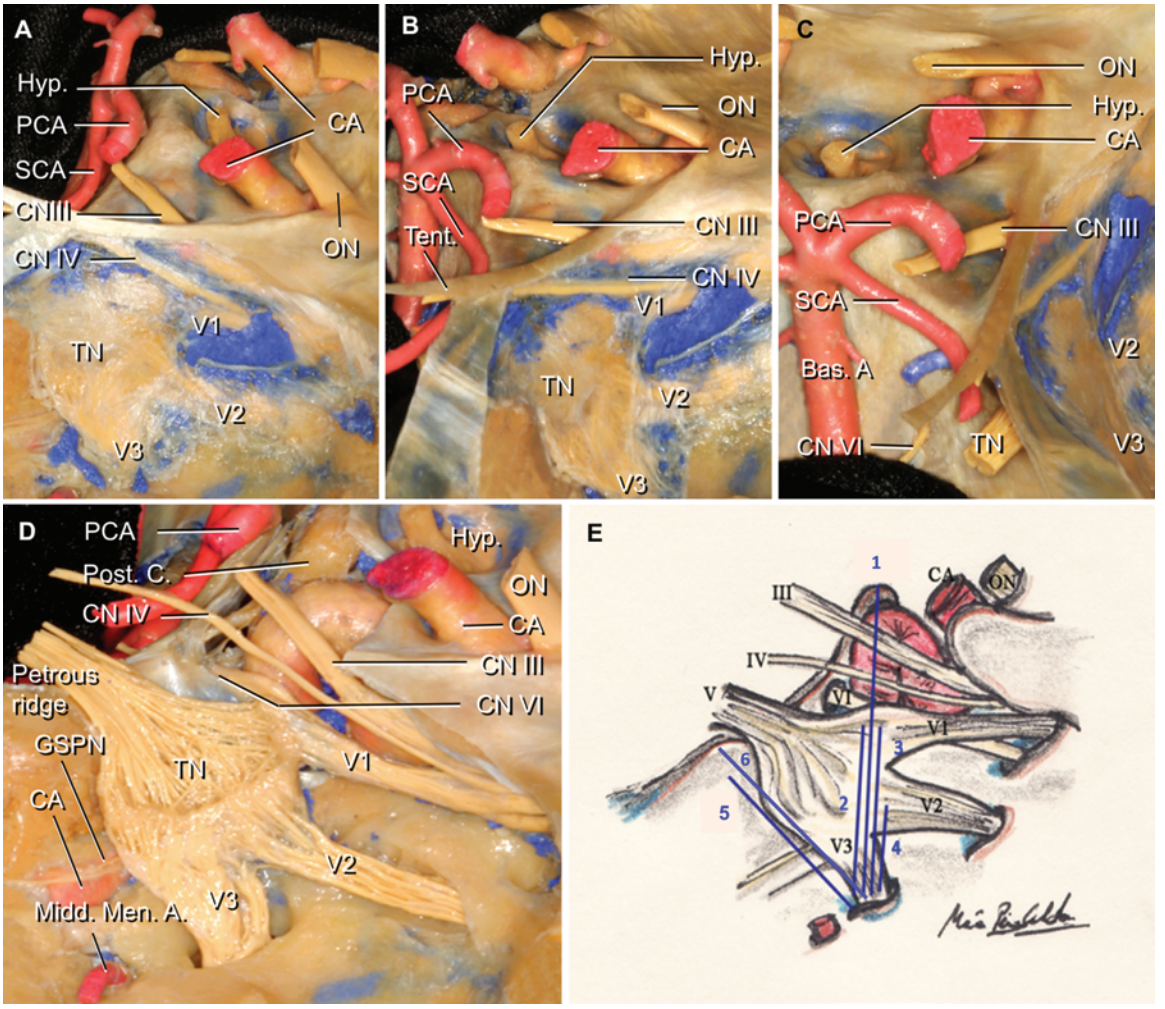

Fig. 2. Photographs showing dissection of the Meckel cave and cavernous sinus on the right side. **A–C:** Lateral (A), oblique (B), and posterior (C) views of the Meckel cave and cavernous sinus with the periosteal layer of the dura mater intact. **D:** Dissection after removing the periosteal layer of the dura mater. **E:** Illustration showing measurements in the middle fossa: 1 = distance from the FO to the posterior clinoid process; 2 = distance from the FO to the exit of the internal carotid artery from the petrous bone (not shown); 3 = distance from the FO to the middle part of V1 in the FO–posterior clinoid line; 4 = distance from the FO to the middle part of V2 in the FO–posterior clinoid line; 5 = distance from the FO to the common root of the TN in the middle fossa; 6 = distance from the middle part of the FO to the petrous ridge. Bas. A = basilar artery; CA = internal carotid artery; CN = cranial nerve; GSPN = greater superficial petrosal nerve; Hyp. = hypophyseal gland; Midd. Men. A. = middle meningeal artery; ON = optic nerve; PCA = posterior cerebral artery; Post. C. = posterior clinoid; SCA = superior cerebellar artery; Tent. = tentorium.

patients with trigeminal neuralgia treated by the senior author (R.A.M.) using radiofrequency at Vanderbilt University Medical Center were assessed. Only those patients with more than 6 weeks of follow-up were studied. The data considered included age, sex, side of trigeminal neuralgia pain, trigeminal neuralgia pain distribution (with V1 involvement/without V1 involvement), and the presence or absence of multiple sclerosis or complications. The degree of pain relief within the first 6 postoperative weeks ranged from complete pain relief to facial pain or the need to increase medications.

Patients were placed supine and general anesthesia was induced using intravenous methohexital. After identifying the FO in the oblique-inferior view, a standard radiofrequency needle was percutaneously advanced directly through the face, approximately 3 cm lateral to the oral commissure, to reach the retrogasserian portion of the TN. The stylet was removed, and an electrode was inserted in its place. The patient was then allowed to waken, and stimulation was performed to confirm that the electrode was positioned in the desired TN division. The anesthesia was then deepened to begin the radiofrequency lesioning (70° for 60 seconds). If the patient continued to experience sharp pain, the procedure was repeated until facial sensation was less than 50% of the untreated side. Typically, when the branch involved was V1, the lesioning was started at 60° and repeated until the sensation was below the 50% criteria. After testing the facial sensation, the stylet was removed and pressure was applied until adequate hemostasis was achieved.

Differential FO Puncture

A temporal craniectomy, lobectomy, and Meckel cave dissection were performed in 6 sides of 4 formalin-

TABLE 2: Anatomy of the FO and surrounding areas*

Measurement (mm)†	No. of Specimen Sides	Minimum	Maximum	Average	Standard Deviation
FO–Pclin (1)	32	23.00	34.00	28.5781	2.99760
FO–carotid (2)	36	8.00	16.50	11.5833	2.20875
FO–V1 (3)	36	10.00	19.00	14.5694	1.87903
FO–V2 (4)	36	6.50	12.00	9.1667	1.31475
FO–common root V (5)	26	12.00	19.00	16.0192	1.74631
FO–petrous ridge (6)	34	15.00	24.00	19.5588	2.03293
Meckel cave depth	36	2.00	6.00	4.0278	1.04843
FO–int. cant. lig.	36	6.00	20.00	12.7778	3.14517
FO–post. trag.	26	15.00	35.00	27.9038	4.37269

* FO–Pclin = distance from the FO to the posterior clinoid process; FO–carotid = distance from the FO to the exit of the internal carotid artery from the petrous bone; FO–V1 = distance from the middle portion of the FO to the middle portion of V1 in the FO–Pclin line; FO–V2 = distance from the middle portion of the FO to the middle portion of V2 in the FO–Pclin line; FO–common root V = distance from the FO to the common root of the fifth cranial nerve in the middle fossa; FO–petrous ridge = distance from the FO to the petrous ridge; FO–int. cant. lig. = distance from the projection of the FO to the internal canthal ligament; FO–post. trag. = distance from the posterior portion of the tragus to the projection of the FO in the lateral view.

† Numbers in parentheses correspond to the measurements represented in Fig. 2E.

fixed, silicone-injected specimens. The 40°–45° inferior transfacial–20° oblique projections allowed visualization of the FO. Radiofrequency needles, with Tew electrodes (straight and curved; Cosman), were inserted under fluoroscopic guidance at distances +5 mm, 0 mm, and –5 mm from the clival line in the lateral radiographic view in the medial, middle, and lateral third of the FO. The TN branches covered with the electrode tip were confirmed by direct visualization.

Statistical Analysis

Descriptive and analytical studies were performed using SPSS software (version 18, IBM).

Results

Trajectory to the FO

To reach the FO, a needle is inserted between the buccinator and masseter muscles in the fat-filled space located 2.5–3 cm lateral to the oral commissure. Care should be taken not to perforate the oral mucosa by placing the index finger inside the mouth, thereby protecting the needle from medial misplacement. The facial vein, and less frequently facial artery (anterior to the vein), may be encountered, which can result in postoperative facial hematomas. The Stensen duct is in the path of the needle, so it is possible to damage it; we did not find a constant reference to avoid its damage (Fig. 4).

With deeper penetration of the needle, the internal maxillary artery and pterygoid venous plexus lie in the path of the needle at the level of the pterygoid muscles and can be a source of postoperative hematomas. The V3 branches are encountered in this area: the buccal nerve, located between the 2 fascicles of the lateral pterygoid muscle; the lingual and inferior alveolar nerves, located between the lateral and medial pterygoid muscles; and the auriculotemporal nerve, which is located behind the mandible and in front of the tragus. Some of the motor branches in this area lie over the bone: the masseteric nerve over the mandible behind the masseter muscle, and the deep temporal nerves over the temporal bone behind the temporalis muscle. All of these branches converge onto the FO (Fig. 5). To reach the FO, the lateral pterygoid muscle has to be pierced. The TN in the middle fossa is located in the Meckel cave over the anterior portion of the petrous part of the temporal bone.

Anatomical Relationships of the FO: Measurements in Dry Skulls and Formalin-Fixed Specimens

The FO is an elliptical-shaped (Fig. 1), short, osseous canal in the middle fossa of the skull base, with a 7-mm major diameter and a 4-mm minor diameter (Table 1), located approximately 2 mm behind the pterygoid base. It is located in a sagittal plane that passes through the midpupillary line (13 mm lateral to the internal canthal ligament). The FO is 28 mm anterior to the posterior limit of the tragus. The FO is situated approximately at the level of the posterior root of the zygomatic arch. Its orientation is oblique, with its major axis anteromedial to posterolateral. Distances from the FO to important structures in the exocranial surface of the skull base are represented in Fig. 1 and Table 1.

The Meckel cave, a 4-mm deep osseous depression in the petrous bone that contains the gasserian ganglion, is located in the middle fossa of the skull base. To measure distances in the middle fossa of formalin-fixed specimens, a line between the middle point of the FO and the posterior clinoid process was considered (Fig. 2, Table 2). The posterior clinoid process is located posterior to the FO in 77.4% of cases, anterior in 19.4%, and at the same plane in 3.2%. The cavernous carotid artery is located 11.6 mm from the FO on this line. In our specimens, the average distance from the FO to the petrous ridge was approximately 20 mm (range 15–24 mm). Only 3.55 mm of the common root of the TN was located in

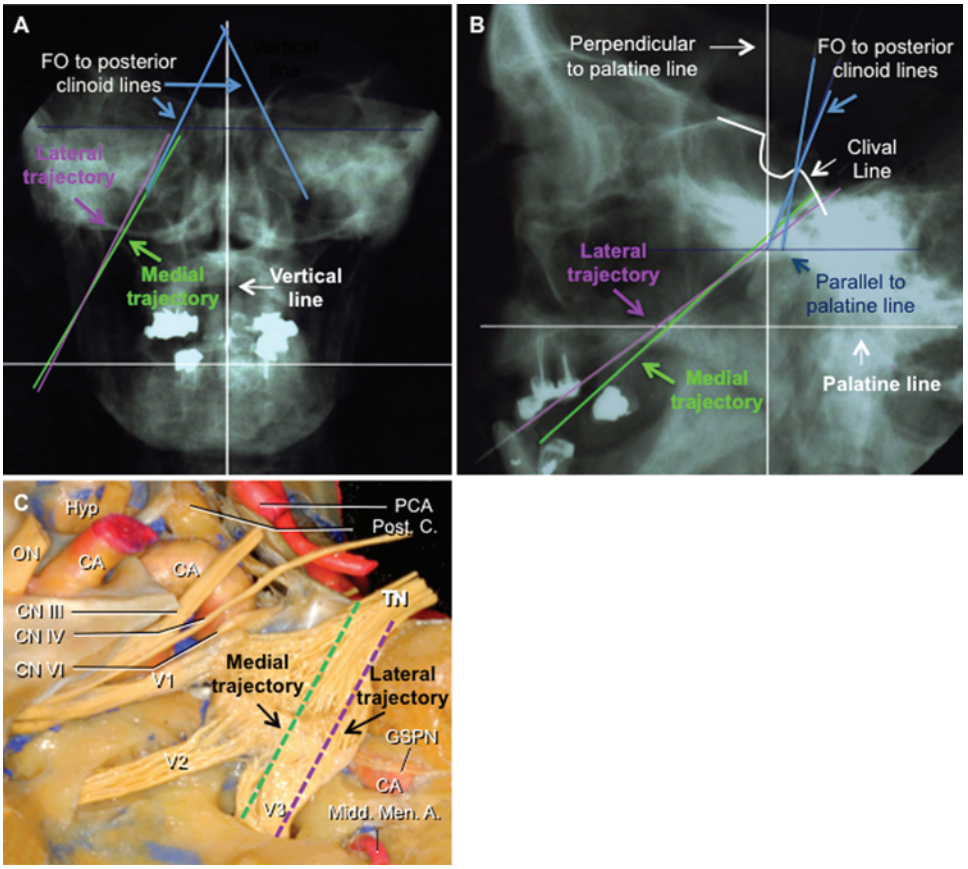

Fig. 3. Anteroposterior **(A)** and lateral **(B)** radiographic views of the different angles and trajectories of the FO puncture in specimens. The trajectories were studied after insertion of lumbar puncture needles and have been highlighted with different colors. Two extradural trajectories were measured: 1) the medial trajectory, represented by a *green line* passing through the retrogasserian portion in the medial part of the common root of the TN in the trigeminal impression of the petrous ridge, and the medial part of the FO; and 2) the lateral trajectory, represented by a *purple line* passing through the lateral part of the common root of the TN in the trigeminal impression of the petrous ridge, and the lateral part of the FO. A shorter needle was placed between the FO and posterior clinoid process for additional measurements *(blue lines)*. **C:** Photograph showing dissection of the cavernous sinus and Meckel cave, in which the medial and lateral trajectories have been represented. CA = carotid artery; CN = cranial nerve; GSPN = greater superficial petrosal nerve; Hyp = hypophyseal gland; Midd. Men. A. = middle meningeal artery; ON = optic nerve; PCA = posterior cerebral artery; Post. C. = posterior clinoid.

the middle fossa over the petrous bone. With the aim to define the safety distance for avoiding cavernous carotid artery puncture, the distance from the theoretical position of the petrolingual ligament (lingual process of the sphenoid bone) to the midline was measured in 40 dry skulls. This distance ranged from 13 mm to 18 mm (mean 15.22 mm; Fig. 6). It was possible to puncture the carotid artery in the cavernous sinus in 29 (36.7%) of 79 skull sides using a more lateral-to-medial and posterior-to-anterior puncture. It was also possible to puncture the carotid artery in the horizontal petrous segment in 24 (30.4%) of 79 skull sides. The entry point to puncture the artery at this level would be located far superior to the ideal entry point in the cheek, almost touching the zygomatic bone. This makes damage to the carotid artery at this point unlikely (Fig. 6D and E). The portion of the horizontal petrous segment of the carotid artery not covered by bone was lateral to the Meckel cave in 72.5% of skulls, in the middle portion of the Meckel cave in 17.5%, and was completely covered up to the petrolingual ligament in 10%.

Visualizing the FO on Radiography

In 96.2% of the skull sides, the FO was visualized in a 40°/45° inferior transfacial–20° oblique projection. In 3.8% of cases (3 sides, 2 skulls), the FO was not visualized in any position of the radiograph. Regarding the transfacial angle, in 70 (88.6%) of 79 skull sides the FO was visualized in the 40° projection, in 13 skull sides the transfacial angle was increased up to 45° to visualize or improve visualization of the FO, and in only 2 sides was the visualization better with a 35° projection. Regarding the oblique angle, in 76 (96.2%) of 79 skull sides the FO was visualized in the 20° oblique projection, although in some of them (6 sides) visualization improved with 30°–35° projection (Fig. 7).

Medial and Lateral Trajectories of the FO Puncture

The ideal trajectory of the needle puncture was calculated after the study of the medial and lateral trajectories as described in the *Methods* (Fig. 3, Table 3). The medial trajectory from the medial aspect of the FO to the medial

TABLE 3: Measurements of distances and angles of the specimens in the lateral and medial trajectories to reach the retrogasserian portion of the TN*

Measurement	No. of Specimens	Minimum	Maximum	Average	Standard Deviation
angles (°)					
angle AP lat. traj.-vert.	17	13.50	28.00	21.0294	3.31884
angle lat. traj.-palate (lat)	17	34.00	58.00	44.7647	6.60047
angle AP med. traj.-vert.	17	16.00	28.00	21.2941	3.42353
angle med. traj.-palate (lat)	17	32.00	62.00	48.1176	7.30481
angle AP vert.-FO Pclin.	31	20.00	47.00	33.1290	6.63698
angle vert.-FO Pclin. (lat)	31	0.00	21.00	9.4516	5.50054
distances (mm)					
lat. traj. X	17	10.00	35.00	26.0000	5.87367
lat. traj. Y	17	−5.00	10.00	1.0588	4.56167
med. traj. X	17	15.00	35.00	24.4118	5.59083
med. traj. Y	17	−15.00	7.00	−3.6471	5.94707
AP lat.-med.	16	1.71	6.46	3.06	1.10
lat.-med. (lat)	17	0.86	5.14	2.78	1.10
med. traj.-inf. shadow	15	19.2	28.61	22.34	2.52
lat. traj.-inf. shadow	16	20	28.61	23.72	2.37
med. traj.-midline	15	15.4	22.15	18.88	2.28
lat. traj.-midline	15	18	25	22.03	2.31
med. traj.-clival	10	1.78	9.23	4.47	2.22
lat. traj.-clival	11	4	10.15	6.33	1.88
med. traj. tip-inf. sella	16	0	3.69	1.33	1.32

* Angle AP lat. traj.-vert. = angle between the lateral trajectory and a vertical line in the AP radiographic view; angle lat. traj.-palate (lat) = angle between the lateral trajectory and the palatine line in lateral radiographic view; angle AP med. traj.-vert. = angle between the medial trajectory and a vertical line in the AP radiographic view; angle med. traj.-palate (lat) = angle between the medial trajectory and the palatine line in lateral radiographic view; angle AP vert.-FO Pclin. = angle in the AP radiographic view between a vertical line and the FO-to-posterior clinoid line; angle vert.-FO Pclin. (lat) = angle in the lateral radiographic view between a vertical line and the FO-to-posterior clinoid line; lat. traj. X = lateral distance from the needle to the oral commissure in the lateral trajectory; lat. traj. Y = superior-inferior distance from the needle to the oral commissure in the lateral trajectory; med. traj. X = lateral distance from the needle to the oral commissure in the medial trajectory; med. traj. Y = superior-inferior distance from the needle to the oral commissure in the medial trajectory; AP lat.-med. = distance between both trajectories in the AP radiographic view at the level of the petrous ridge; lat.-med. (lat) = distance between both trajectories in the lateral radiographic view at the level of the petrous ridge; med. traj.-inf. shadow = distance from the tip of the medial trajectory to the inferior shadow of the middle fossa in the lateral view; lat. traj.-inf. shadow = distance from the tip of the lateral trajectory to the inferior shadow of the middle fossa in the lateral view; med. traj.-midline = distance from the tip of the medial trajectory in the petrous ridge to the midline; lat. traj.-midline = distance from the tip of the lateral trajectory in the petrous ridge to the midline; med. traj.-clival = distance from the tip of the medial trajectory to the clival line in the lateral view; lat. traj.-clival = distance from the tip of the lateral trajectory to the clival line in the lateral view; med. traj. tip-inf. sella = distance from the tip of the medial trajectory to a line parallel to the palatine line that passes inferiorly to the sella.

aspect of the common root of the TN projects through the retrogasserian portion of V2 and V1. This trajectory has an entry point 24.4 mm lateral and 3.6 mm inferior to the oral commissure and, in the lateral view, has an angle of 48.11° superior to the hard palate. This angle is 21.29° medial in the AP radiograph.

The lateral trajectory, from the lateral third of the FO to the lateral portion of the common root of the TN, projects through the retrogasserian portion of V3. This trajectory has an entry point 26 mm lateral and 1.06 mm superior to the oral commissure, and in the lateral view has an angle of 44.76° superior to the hard palate. This angle is 21.02° medial in the AP radiograph.

None of these measurements were significantly different between the 2 trajectories, which are almost parallel. This parallelism depends on the size of the FO and the width of the common root of the TN over the trigeminal impression. The approximate angles for the needle insertion would be 45° with the hard palate in the lateral radiograph and 20° medially in the AP radiograph.

As the needles were inserted through the FO up to the posterior limit of the petrous ridge, the distance between the clival line and the tip of the needle was measured for the lateral and medial needle trajectories. The clival line was defined as the major radiopaque line that runs posteriorly and follows the line surrounding the anterior, inferior, and posterior margins of the sella. Because the petrous ridge has a posterior angulation, the distance from the petrous ridge to the clival line was always greater in the lateral puncture, therefore the safe distance from the needle tip to the clival line increases from medial to lateral. The distance from the clival line (n = 10) to the tip of the needle in the medial trajectory ranged from 1.78 mm to 9.23 mm, with an average of 4.47 mm. This distance in the lateral trajectory ranged from 4 mm to 10.15 mm, with an average of 6.33 mm, and the

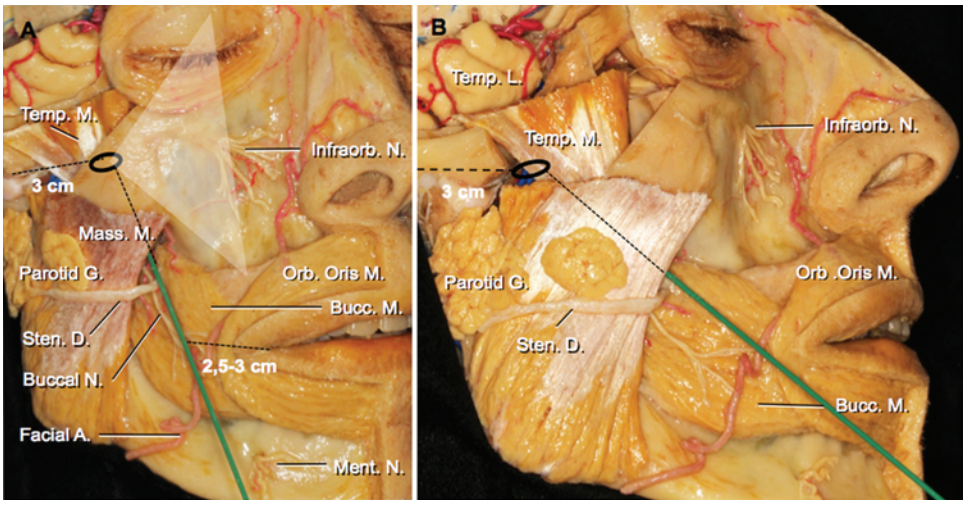

Fig. 4. Photographs showing FO puncture and anatomical dissection of the percutaneous route. **A:** Oblique view. To reach the FO *(black oval)*, the needle should be placed from the entry point, 2.5–3 cm lateral to the oral commissure to the intersection of a coronal plane 3 cm anterior to the tragus, a sagittal plane in the medial pupillary line, and an axial plane parallel to the skull base (Harthel technique). **B:** Trajectory of the needle to reach the FO *(black oval)* in the lateral view. In this specimen, the zygomatic arch, the squamous part of the temporal bone, and the lateral wall of the orbit have been removed. Bucc. M. = buccinator muscle; Facial A. = facial artery; Infraorb. N. = infraorbital nerve; Mass. M. = masseter muscle; Ment. N. = mentonian nerve; Orb. Oris M. = orbicularis oris muscle; Parotid G. = parotid gland; Sten. D. = Stensen duct; Temp. M. = temporalis muscle; Temp. L. = temporal lobe.

average between the medial and lateral distance, representing a puncture in the midportion of the FO, was 5.37 mm. Based on these measurements, a safe distance of the needle tip to the clival line on a direct lateral radiographic projection would be approximately 2 mm when entering the FO medially and 4 mm when entering the most lateral portion. For a midpoint entry, the safe distance calculated is approximately 3 mm. When placing electrodes to register the mesial temporal activity through the FO, the trajectory is the same, but the dura mater has to be pierced (the anterior part of the tentorium attached to the petrous ridge) to enable the electrode to reach the ambient cistern and contact the mesial part of the temporal lobe. A more vertical trajectory that goes through the middle fossa dura mater could easily damage the temporal lobe. A deeper and more medial trajectory can injure the third, fourth, and sixth cranial nerves, the brainstem, and vascular structures, including the cavernous carotid artery and posterior cerebral artery among others.

Clinical Outcomes

The data recorded in 57 patients were age (mean 68.29 ± 11.10 years, range 44–86 years), sex (17 men, 40 women), side (right 34, left 23), and presence of multiple sclerosis (10 patients). In the 49 patients who had more than 6 weeks of recorded follow-up, acute pain relief was found in 97.95%; almost all patients felt less pain after the surgery. Strict criteria were used to distinguish among different outcomes. Neuralgia in V1 was significantly correlated with the presence of facial pain or the need to increase medication in the first 6 weeks postoperatively compared with patients who suffered from V2 and/or V3 neuralgia ($p = 0.001$, Fisher exact test). Age, sex, side, and multiple sclerosis were not significantly correlated with worse outcome in this series. Four of 57 patients experienced complications: meningitis (n = 1), painful anesthesia (n = 1), postoperative hematoma without clinical significance (n = 1), and corneal anesthesia associated with a V2 procedure (n = 1). In 3 patients, the visualization of the FO was difficult in transfacial-oblique radiographic fluoroscopy, and 1 patient required CT neuronavigation.

Foramen Ovale Puncture in Different Parts of the FO in Anatomical Specimens

The 40°/45° inferior transfacial–20° oblique position allowed us to visualize and select the part of the FO to be punctured and was confirmed with direct intracranial visualization. After correct needle insertion, approximately 45° superior and 20° medial directed to the petrous ridge, the needle was advanced from the medial, middle, and lateral parts of the FO, situating the electrode tip at +5, 0, and –5 mm from the clival line. There were 3 tip positions in each puncture: a Tew electrode curved up and medial, a Tew electrode curved inferior and lateral, and a straight Tew electrode. Each position of the electrode was counted as a puncture. The complete length of the electrode tip was considered to confirm anatomical location. The success rate was higher for V1 if the needle was inserted in the medial part of the FO beyond the clival line, for V2 in the middle part beyond the clival line, and for V3 in the lateral part beyond the clival line (Table 4, Fig. 8). At –5 mm, most of the punctures were located in the gasserian ganglion of the TN. Few punctures were anatomically exclusive for V1 and this situation was more frequent for V3.

Discussion

How to Reach the FO

When performing the classic transovale approach for

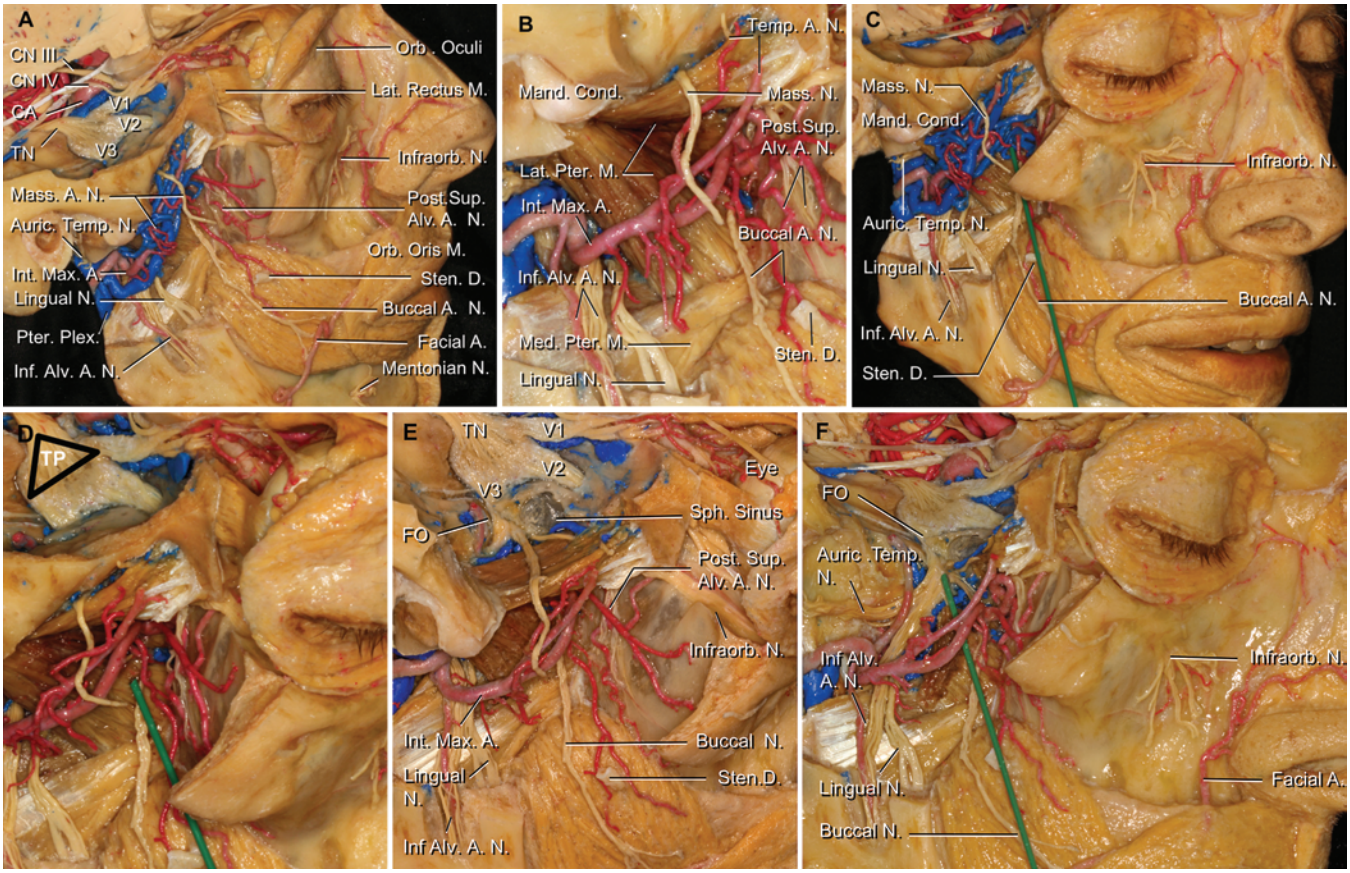

Fig. 5. Dissection of the infratemporal fossa after removal of the ascending ramus of the mandible, masseter, and temporalis muscles. The middle cranial fossa and orbit have been dissected. **A:** The internal maxillary artery and pterygoid venous plexus are seen in depth, as well as V3 branches (buccal, lingual, inferior alveolar, masseteric, deep temporal, and auriculotemporal nerves). The lateral and superior walls of the orbit have been removed to show the relationship of the middle fossa with the orbit through the superior orbital fissure, and the infratemporal fossa with the orbit through the inferior orbital fissure. After removing the temporal lobe and dura mater of the middle fossa and cavernous sinus, the TN is shown as well as its relationships with the third and fourth cranial nerves and the carotid artery. **B:** Closer view of the infratemporal fossa, in which the pterygoid venous plexus has been removed to show the internal maxillary artery and its branches. **C:** Oblique view of the same dissection with the needle inserted pointing toward the retrogasserian part of the TN. **D:** Closer view of the TN in the Meckel cave, cavernous sinus, and their relationship with the orbit and infratemporal fossa. The *triangular area* shows the triangular plexus (TP), the retrogasserian portion of the TN in the Meckel cave. **E:** Dissection of the middle fossa and deep infratemporal fossa. View after drilling the middle fossa floor up to the FO and the anterolateral triangle of the middle fossa. The sphenoid sinus has been opened. **F:** After the resection of the lateral pterygoid muscle, V3 branches from the FO can be visualized. The Stensen duct, internal maxillary artery, and pterygoid venous plexus might be in the path of the needle. A = artery; Auric. Temp. N. = auriculotemporal nerve; Buccal A. N. = buccal artery and nerve; CA = carotid artery; CN = cranial nerve; Inf. Alv. A. N. = inferior alveolar artery and nerve; Infraorb. N. = infraorbital nerve; Int. Max. A. = internal maxillary artery; Lat. Rectus M. = lateral rectus muscle; Lat. Pter. M. = lateral pterygoid muscle; Lingual N. = lingual nerve; Mand. Cond. = mandibular condyle; Mass. A. N. = masseteric artery and nerve; Med. Pter. M. = medial pterygoid muscle; N. = nerve; Orb. Oculi = orbicularis oculi muscle; Orb. Oris = orbicularis oris muscle; Post. Sup. Alv. A. N. = posterior superior alveolar artery and nerves; Pter. Plex. = pterygoid venous plexus; Sph. Sin. = sphenoid sinus; Sten. D. = Stensen duct; Temp. A. N. = deep temporal artery and nerve.

percutaneous trigeminal rhizotomy, the needle is inserted 2.5–3 cm lateral to the labial commissure. The needle is then advanced toward the point of intersection between a coronal plane positioned 3 cm anterior to the tragus and a sagittal plane through the medial ipsilateral pupil. At the skull base in the greater wing of the sphenoid bone, the needle is inserted through the FO. The location of the FO cannot be visualized using uniplanar fluoroscopy. Additionally, detecting the FO in the purely submental view can be difficult.[11,14,18] Multiple groups have previously studied the optimal angles for FO visualization. In the submental modified view, inferior transfacial and oblique angulations vary from 15°–70° transfacial and 15°–25° oblique.[1,9,11,12,44,49] The FO was optimally visualized in most of the skulls with a radiographic angulation of 40°/45° inferior transfacial projection and 20° oblique projection. An interesting radiographic sign, called "the setting sun sign," was observed in most of the skulls by centering the inferior transfacial angle at 40° or slightly changing it under radiographic magnification. The setting sun sign is the petrous ridge line in the middle of the FO and is used as a landmark to guide the needle to the

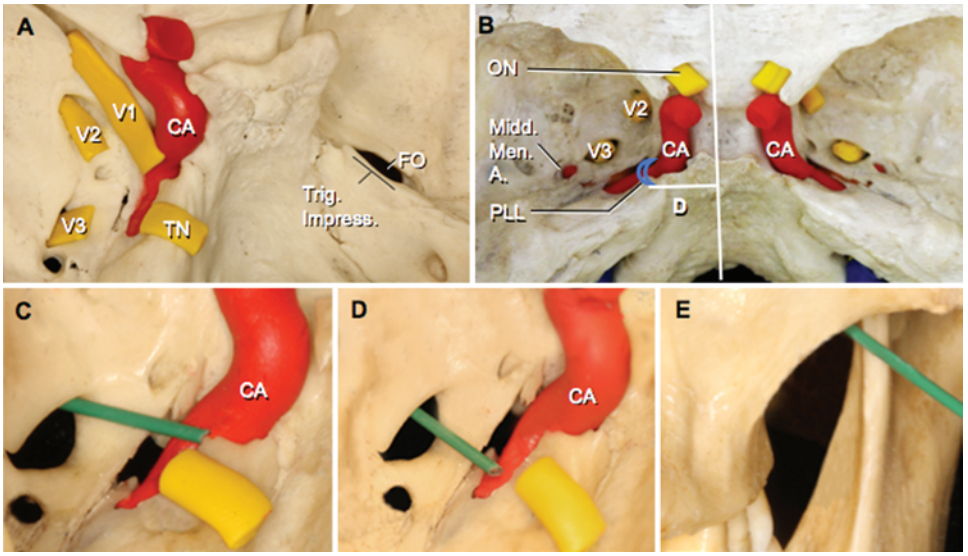

Fig. 6. Photographs showing FO puncture and the internal carotid artery. **A:** Oblique lateral view of a representation with molding material of the carotid artery (CA), V1, V2, and V3 in a dry skull. The retrogasserian portion of the TN lies over the trigeminal impression (Trig. Impress.). **B:** Skull with molding material representing the previous structures and the optic nerve (ON). D = distance from midline to the theoretical location of the petrolingual ligament (PLL) between the petrous bone and the lingual process of the sphenoid bone. Midd. Men. A. = middle meningeal artery. **C:** According to our data, it is possible to puncture the CA in the cavernous sinus in 29 (36.7%) of 79 sides of skulls with an excessive medially directed puncture (shown), which can lead to a carotid-cavernous fistula. **D and E:** It is also possible to puncture the CA in the horizontal petrous segment in 24 (30.4%) of 79 sides of skulls (D), but with an extremely superior entry point in the facial region (shown) almost touching the zygoma (E).

porus trigeminus, which is located in the petrous ridge.[1] In 96.2% of the skulls in our study we could visualize the FO with these angles, and in some cases a change to 35° in any or both angles improved visualization. In cases in which fluoroscopy is not an aid for FO puncture, the anatomical relationships of the FO in the lateral and AP radiographs are essential. Neuronavigation systems may also be required in these patients.[14,20,55]

Numerous causes, such as osteoporosis or dura mater calcifications, have been reported for difficulty with visualization of the FO during fluoroscopy.[9] In addition, our results show that in dry skulls the orientation and length of the FO canal, which is related to the width of the pterygoid base, might add difficulty. A thicker pterygoid base, forming the anterior portion of the FO canal, makes visualization with radiography challenging (Fig. 7). Numerous other causes that are not present in dry skulls may alter these results, making the FO invisible for radiography in a higher percentage than shown in this study.

We confirmed anatomically that the needle has to be inserted approximately 25 mm (range 10–35 mm) lateral to the oral commissure, and directed almost 30 mm (range 15–35 mm) anterior to the tragus and 13 mm (range 6–20 mm) lateral to the internal canthal ligament, just medial to the midpupillary line. These data are consistent with the classic technique for the FO puncture.[18] However, these ranges are too large to establish a concrete external reference that depends on the facial structure of the soft tissue. Moreover the needle, once inserted, can be moved widely within the soft tissue, changing its orientation so the bone structures can be more reliable reference points. In cases in which the FO is not visualized, osseous structures can be used as reference points to avoid multiple needle punctures. The FO is located slightly lateral to the posterior base of the pterygoid process of the sphenoid bone (2.3 mm), and can be reached through a puncture strictly parallel to midline with the needle as close as possible to the maxilla. The pterygoids are posterior and medial to the most prominent aspect of the maxilla laterally. Hence, after the insertion, the needle can be directed as close as possible to the maxilla, parallel to the midline, toward the posterior base of the pterygoid process. If the FO has not been entered at this time, the needle can be safely advanced over the extracranial skull base up to 8 mm posteriorly (the inferior limit of the distance from the FO to the carotid foramen) and 3.5 mm medially (the inferior limit of the distance from the FO to the foramen lacerum) to avoid complications due to the carotid artery extracranial puncture. In only 1 of 77 skull sides, the FO was positioned more than 8 mm posterior to the pterygoid base, and in 10 of 90 skull sides, the FO was located more than 3.5-mm medial to the pterygoid base (Fig. 1, Table 1). Immediately after reaching the FO, the angles can be adjusted to accomplish a correct trajectory. A correct puncture is parallel to the Meckel cave in the direction toward the porus trigeminus, approximately 45° superior to the hard palate in the lateral view and 20° medial in the AP view. These measurements are coincident with the results obtained for optimal visualization of the FO in radiographs in dry skulls. Our angles are different than those published by Tatli and Sindou,[43] most likely due to the use of the orbitomeatal line as a reference in their study instead of the hard palate that we considered an easier reference.

Complications and Anatomy

Numerous complications have been reported as a re-

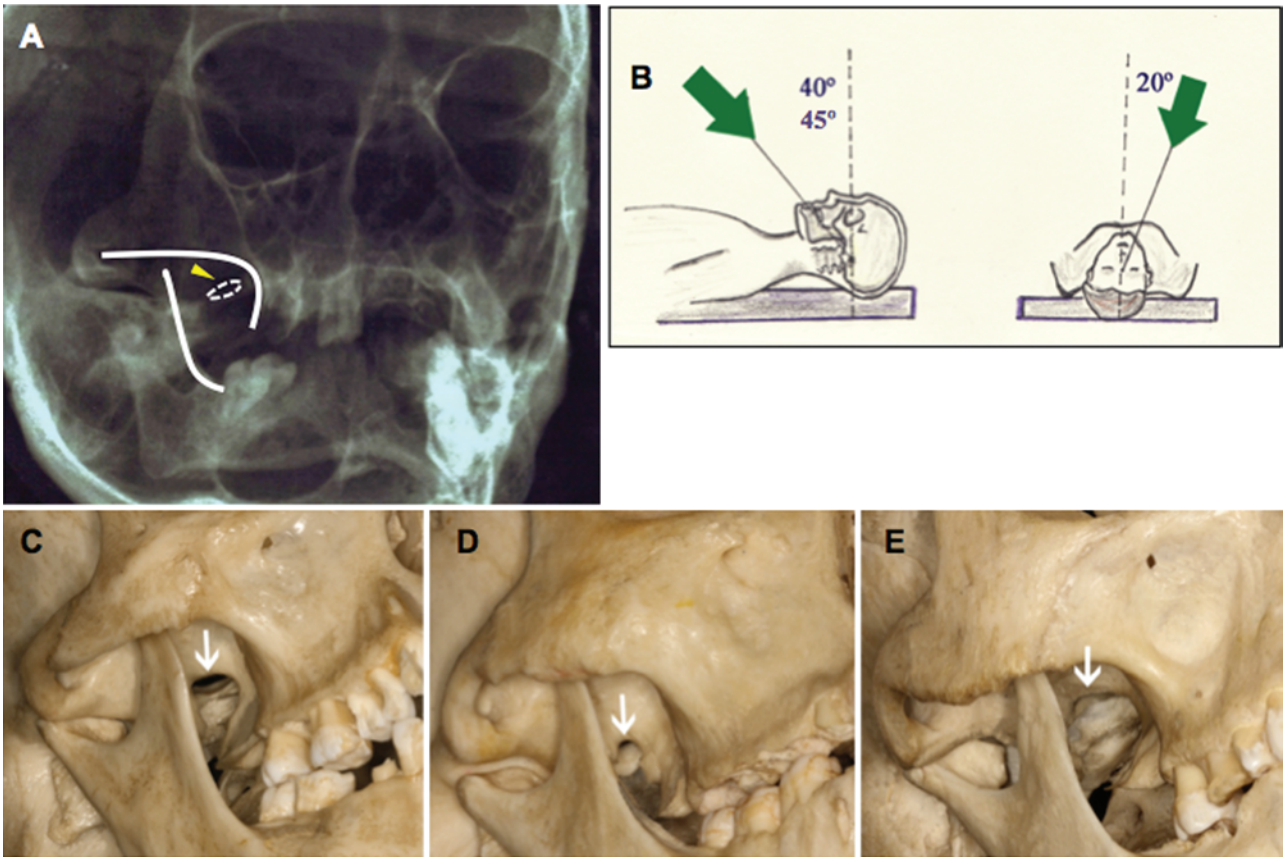

Fig. 7. Visualization of the FO using radiography. **A:** Radiographic view of the 40°/45° inferior transfacial–20° oblique projection. The FO *(dashed elliptic shape, yellow arrow)* can be identified between the line formed by the inferior line of the zygoma-maxilla and the anterior line of the mandible. Adjusting the transfacial angle, the setting sun sign might be observed (line of the petrous ridge in the middle of the FO, not shown). **B:** Graphic illustration of these angles. **C–E:** Anatomical correlation of the radiograph visualizing the FO *(arrows)* in the 40°/45° inferior transfacial–20° oblique view in different anatomical types. In the most common view of the FO (C), note that the petrous ridge can be observed in the middle of the FO (correlation of setting sun sign). The next image (D) shows a specimen in which the FO was visualized with difficulties in the radiograph corresponding to a narrow, thick osseous canal. In the last image (E), the FO was not observed in any projection of the radiograph in this specimen due to the thickness of the pterygoid base and orientation of the FO canal.

sult of percutaneous access to the FO with both incorrect (Table 5) and correct (Table 6) needle placement.

Injury to Extracranial Structures Due to Incorrect Needle Placement. Blindness has been reported due to needle insertion in the inferior orbital fissure.[5,8] The inferior transfacial-oblique view can give misleading information, as shown in Fig. 9A–C. This incorrect orientation can be avoided with a lateral view that clearly shows the misplaced tip.

It is possible to puncture the internal carotid artery at its entrance in the carotid canal in the temporal bone (at a safe distance of 8 mm posterior to the FO; Fig. 9G–I) as well as the internal jugular vein (at a minimum of 12 mm posterior to the FO; Fig. 9J–L). Injury to the eustachian tube is possible and may lead to transient rhinorrhea. A lateral radiograph and transfacial-oblique view help in detecting the displacement.

Injury to the internal carotid artery is also possible in the exocranial surface of the skull base in the foramen lacerum, which is located on average 6.73 mm medial to the FO and has a minimum distance of 3.5 mm medial to the FO (Fig. 9D–F).

No major complications are due to a pure laterally displaced needle. All surrounding anatomical structures susceptible to be injured by a misplaced tip are visualized in Fig. 10.

Injury to Intracranial Structures Due to Incorrect Needle Placement. Once the needle pierces the FO, numerous complications can arise from the medial or lateral displacement of the needle as well as deeper insertion. A carotid-cavernous fistula is an uncommon but severe complication of the procedure[10,21,24,26,39] and can be related to a tip displaced medial to the petrolingual ligament. In our study, the safe region would be more than 18 mm from midline in the AP view, and was 18 mm in only 1 (1.26%) of 79 skull sides, but the average distance from the petrolingual ligament to midline was 15.55 mm. The average distance from the midline to the medial trajectory was 18.88 mm and to the lateral trajectory was 22.03 mm. Moreover, the cavernous carotid artery puncture was not possible in 62.4% of specimens, in which the mandible was an obstacle to directing the needle more medially. Although the petrous portion of the internal carotid ar-

TABLE 4: Punctures at +5, 0, and –5 mm from the clival line in the medial, middle, and lateral portions of the FO in anatomical specimens*

Puncture (mm)	V1	V1/Total (%)	V1 Only	V1 Only/V1 (%)	V2	V2/Total (%)	V2 Only	V2 Only/ V2 (%)	V3	V3/Total (%)	V3 Only	V3 Only/ V3 (%)	GASS	Total
MED +5	11	**73.33**	2	18.18	12	80	2	16.67	6	40	3	50	0	15
MID +5	5	38.46	1	20	11	**84.61**	3	27.27	7	53.84	1	14.28	0	13
LAT +5	2	18.18	0	0	4	36.36	0	0	11	**100**	7	63.63	0	11
MED 0	2	12.5	1	50	9	56.25	2	22.22	10	62.5	6	60	0	16
MID 0	2	15.38	0	0	6	46.15	1	16.67	8	61.53	4	50	0	13
LAT 0	0	0	0	0	3	27.27	1	33.33	9	81.81	7	77.77	1	11
MED –5	0	0	0	0	2	11.76	0	0	6	35.29	4	66.67	11	17
MID –5	0	0	0	0	1	7.14	0	0	3	21.42	2	66.67	11	14
LAT –5	0	0	0	0	0	0	0	0	0	0	0	0	11	11

* Total = number of punctures counted in each position with the curved tip up, curved tip down, and the straight tip of the Tew electrode for radiofrequency lesioning; V1, V2, V3 = number of punctures with the electrode anatomically situated in V1, V2, or V3; V1/Total, V2/Total, V3/Total = percentage of the punctures with the electrode located in V1, V2, or V3 out of the total punctures; V1 Only, V2 Only, V3 Only = number of punctures situated exclusively in V1, V2, or V3; V1 Only/V1, V2 Only/V2, V3 Only/V3 = percentage of the exclusive locations in V1, V2, or V3 out of the V1, V2, or V3 locations of the electrode. If the electrode tip was located in the gasserian ganglion, the puncture was counted in the total but as 0 regarding anatomical location in a TN branch. The best results are highlighted in boldface: V1 is better lesioned with a puncture in the medial portion of the FO, V2 in the middle, and V3 in the lateral portion, all of them away (+5 mm) from the clival line. Note that in most punctures, there is more than 1 TN branch involved in contact with the electrode. Abbreviations: GASS = gasserian ganglion; LAT = lateral; MED = medial; MID = middle.

tery is unroofed in most patients and could be a location of internal carotid artery puncture, the needle trajectory needed to access this region is unlikely using the transfacial puncture of the FO. The most injured cranial nerve during rhizotomy is the abducens nerve, with an occurrence of 0.75% in one series.[21] Its anatomical location is adjacent to the petrolingual ligament, lateral to the carotid artery, and behind V1 (Fig. 2). Overall, 13.5% of abducens nerves show a duplicate pattern with different relationships to the petrosphenoidal ligament, thereby making it easier to damage.[22,31,34,35] In addition, there are vascular anastomoses between the TN and abducens nerve that can impair vascular supply to the abducens nerve when the TN is lesioned.[35] Oculomotor paresis occurs infrequently[21] because it is difficult for the needle to reach the oculomotor nerve from the FO. The oculomotor nerve enters the cavernous sinus lateral and anterior to the dorsum sellae and courses along the lower margin of the anterior clinoid process and the carotid oculomotor membrane. The oculomotor nerve crosses the profile of the clivus on average 7 mm from the tip of the dorsum sellae.[19] A puncture that is too posterior, superior, and medial from the clival line can damage it. The trochlear nerve enters the roof of the cavernous sinus posterolateral to the oculomotor nerve and courses below the oculomotor nerve in the posterior part of the lateral wall, immediately above the ophthalmic nerve. Therefore, the trochlear nerve is more frequently injured after V1 lesioning than after V2 or V3 lesioning.[22,32] The trochlear nerve crosses the clivus 12 mm from the tip of the dorsum.[19] Deeper and more medial punctures can contribute to this palsy.

Brainstem lesioning can only be explained by a deep puncture further than the porus trigeminus. A dolichoectasic basilar artery can also be injured during the puncture if trespassing past this anatomical point. Meningitis, most commonly caused by *Streptococcus pneumoniae,* has been reported with an incidence of 0.15% and can be caused by inadvertent penetration of the needle in the buccal mucosa. Temporal lobe hematoma is directly related to dura mater penetration with the needle and subsequently performing the procedure intradurally. The TN is surrounded by the superior petrosal sinus, and some superior petrosal veins are located in the medial portion of the porus.[16] Injuries to neural structures can be avoided with a less deep puncture, so we consider the safe distance from the needle/electrode tip to the clival line to be almost 2 mm when puncturing in the medial portion of the FO, and 4 mm in the lateral portion. This was the minimum distance found in our specimens from the clival line to the petrous ridge. This suggestion is restrictive as the average is 4.46 mm in the medial part and 6.33 mm in the lateral part. These measurements are consistent with the Tew technique that proceeds 5 mm further from the clival line in the middle portion of the FO to reach V1,[46] although in some patients, the tip might be away from the petrous ridge.

Injury to Extracranial Structures With Correct Needle Placement. Alterations of salivation or bloody saliva result from puncturing the Stensen duct. We did not find an anatomical basis to avoid this potential complication.

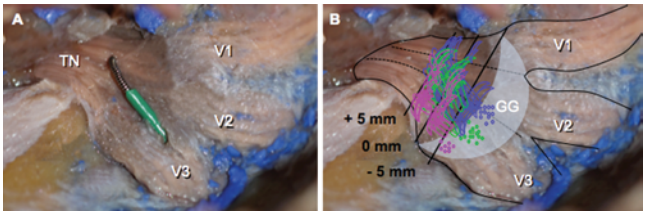

Fig. 8. Puncture in the medial, middle, and lateral thirds of the FO. **A:** Puncture in the middle part of the FO with the electrode curved up at +5 mm from the clival line. Note that the electrode anatomically misses most V1 fibers. Further advancement of the needle would probably not allow the complete lesioning of V1 fibers, whereas a more medial puncture within the FO would probably be more efficient in targeting V1. **B:** Graphic representation in a photograph of the TN of all the punctures performed in different anatomical specimens. Three parts of the FO were studied (medial, middle, and lateral) with the electrode tip located at +5, 0, and –5 mm from the clival line visualized on radiography, with curved Tew electrode up and down (quarter moon shape) and the straight electrode (long oval shape). The punctures performed in the medial portion are represented in *blue*, punctures in the middle portion in *green*, and in the lateral portion of the FO in *red*. *Dots* represent when the electrode was anatomically located in the gasserian ganglion (GG, *shaded*) of the TN. At –5 mm from the clival line, most electrodes were anatomically located in the gasserian ganglion. Note that the medial puncture reached V1 more efficiently than middle and lateral punctures.

With a puncture 2.5 cm lateral to the oral commissure, the duct may be in the needle path as it passes between the buccinator and masseter muscles, located immediately anterior to the Bichat fat pad. Stepwise dissection has shown that the internal maxillary artery and pterygoid plexus might be encountered en route to the FO in the infratemporal fossa. Therefore, the puncture can cause perioperative facial hematomas and, rarely, internal maxillary artery arteriovenous fistulas.[25] The internal maxillary artery has numerous variations in which it can be superficial or deep to the lateral pterygoid muscle, indicating that there are not reliable landmarks to avoid these structures.

Injury to Intracranial Structures With Correct Needle Placement. Impaired hearing can result from tensor tympani nerve injury (a motor branch of the TN) occurring during the coagulation procedure and can be as high as 26.7%.[29] The tensor tympani muscle is located in the floor of the middle fossa parallel to the greater superficial petrosal nerve and can also be uncovered and damaged. Lesioning of the greater superficial petrosal nerve because of compression, thermal injury, or chemical lesioning could explain alterations in lacrimation and nasal secretion described in large patient series.[17,29] The greater superficial petrosal nerve crosses V3 close to the gasserian ganglion and can be easily damaged (Fig. 2). Neuroparalytic keratitis, secondary to the V1 deficit that impairs corneal sensation with abolition of the corneal reflex, is present in 0%–4% of cases[29,48] and can result in blindness.

Masseter muscle weakness due to injury of the motor branch of the TN is not usually perceived by the patient. The motor root exits the brainstem medial to the sensitive part of the TN and crosses the gasserian ganglion from the medial side of the porus to the medial portion of the FO, posterior to the sensitive portion of the TN. Injury to the motor branch of the TN can lead to temporomandibular joint pain due to the force imbalance. Cardiovascular abnormalities have been reported during procedures regarding FO puncture. The posterior fossa dura mater and the arachnoid membrane can extend to the FO instead of ending at the gasserian ganglion. Cerebrospinal fluid fistulas have been reported in 0.13% of cases.[21–23,36]

TABLE 5: Complications caused by incorrect placement of the needle and how to avoid them

Complications	Anatomical Cause	How to Avoid the Complication
extracranial complications		
blindness	medial & anterior displacement to the inferior orbital fissure	lateral radiographic view after the insertion of the needle
injury to extracranial carotid, jugular vein	posterior displacement of the needle, medial displacement for injury of the internal carotid artery in the foramen lacerum	lateral radiographic view, & correct visualization of the FO in the 40°/45°–20° projection
injury to eustachian tube	posterior displacement of the needle	more lateral & anterior trajectory, correct visualization of the FO in the 40°/45°–20° projection
intracranial complications		
carotid-cavernous fistula	carotid artery injury in the cavernous sinus	the tip of the needle/radiofrequency electrode no less than 18 mm away from midline, AP radiographic view
injury to cranial nerves III, IV, & VI	deep & medial displacement of the needle	tip of the needle/radiofrequency electrode no more than 4 mm away from clival line, & control w/ AP radiographic view
brainstem lesioning	needle tip far from the petrous ridge	tip of the needle/radiofrequency electrode no more than 4 mm away beyond the clival line
hematoma	intradural puncture & temporal lobe injury	avoid piercing the middle fossa dura mater following the petrous bone angle (45° w/ the hard palate) in the lateral radiographic view
meningitis	mostly by oral mucosa puncture	avoidance of buccal mucosa; placing the surgeon's index finger inside the oral cavity

TABLE 6: Possible complications of the FO puncture with a correct anatomical placement of the needle and anatomical cause

Complications	Anatomical Cause
extracranial complications	
alterations in salivation	Stensen duct puncture
facial hematomas, facial arteriovenous fistula	puncture of internal maxillary artery & pterygoid venous plexus
intracranial complications	
reduced hearing	injury to the tensor tympani muscle/nerve (TN motor root)
alterations in lacrimation, nasal secretion	greater superficial petrosal nerve injury
neuroparalytic keratitis	TN V1 damage to corneal fibers
masseter weakness	injury to motor root of TN
bradycardia & hypotension	reflex
CSF fistula	depending on anatomical variations of posterior fossa cisterns

Anatomical Basis of Efficacy and Different Techniques

Three treatments can be performed with FO puncture for trigeminal neuralgia,[27,37,42] and selectivity can be achieved using these 3 techniques. For radiofrequency ablation, the electrode tip location is the key part. For balloon compression, the needle has to reach the FO, and the balloon inflates in the Meckel cave, selective lesions can be performed depending on the localization of the Fogarty catheter. For glycerol rhizotomy, the needle has to be located in the trigeminal cistern, and by varying the volume of metrizamide and glycerol and the head position, selectivity can be achieved.[15]

Radiofrequency Ablation. In our study, V1 lesioning with radiofrequency ablation was less successful with more frequent postoperative facial pain in the first weeks than V2 and/or V3 lesioning. One explanation could be the reduced lesion time and temperature used to prevent corneal complications as reported by Sweet and Wepsic.[41] However, in our patient series, the same end point of 50% reduction in sensation compared with the contralateral TN division was used for all 3 divisions. The senior author (R.A.M.) repeats the lesions more frequently at lower temperatures to achieve V1 anesthesia.

This difference in outcome could also be due to the more difficult anatomical location of V1 for the FO puncture. Anatomical references are important for improving selective lesioning of the TN. Some authors[1] have advocated that for V2 or V3 lesioning, the needle has to pierce one-third of the medial end of the FO, whereas for V1, a more lateral skin insertion of the needle with a more medial insertion into the FO, directed to the medial region of the porus trigeminus, is more efficient. However, most authors[47] do not differentiate the region of the FO. Because V1 retrogasserian fibers are rostromedial in the porus trigeminus, V2 in the middle, and V3 in the caudolateral part[6,7,13,38] according to our anatomical study, we believe that a more lateral-to-medial puncture for V1 is less safe for vascular structures and sometimes is difficult due to the position of the mandible that makes it difficult to direct the puncture medially. With the selective puncture of the medial portion of the FO and advancing the electrode tip 5 mm away from the clivus, we were able to reach V1 in 73.3% of cases, in contrast to 38.46% when puncturing the middle region of the FO. Two almost parallel trajectories were studied with no significant differences in angulation between them through the medial and lateral portions of the FO to define the ideal trajectories for the puncture. An insertion 45° up in relation to the hard palate and 20° medial would be the safest and most efficient in reaching the retrogasserian part of the TN. Our results in specimens show that a medial-third puncture of the FO is more successful for reaching V1, while a midportion puncture is best for V2, and a lateral-third puncture for reaching V3.

Similar to our results, V1 and V2 puncture in the medial part of the FO and V3 in the midportion have been advocated by Onofrio.[33] These authors stated that the insertion of the needle in the lateral part of the FO could be more dangerous because of the risk of temporal lobe injury.[33] However, with correct orientation of the needle, this risk is mitigated. A posterolateral entry point in the FO is not advised by some authors because of the possibility of the electrode lying outside the dural sheath.[41] If, after the removal of the stylet, CSF is obtained and the radiographic landmarks show a correct orientation and trajectory of the needle, according to our study, traversing the external third of the FO could be a very efficient way to lesion V3. Tew et al.[47] reported that V1 is more readily accessed with the electrode tip advanced 5 mm distal to the clival line on lateral radiographs, but in the medial portion of the FO as stated before. As the common root of the TN in the petrous ridge turns down to enter the posterior fossa, a deeper insertion is not useful and increases the potential morbidity significantly. For V2, we found that the efficacy would be better with the electrode tip 5 mm away from the clivus piercing the midportion of the FO instead of leaving it at the level of the clival line as with the standard technique:[45,46] in 84.61% of the cases the electrode was located in V2 with the tip 5 mm away from the clival line, compared with 46.15% at the level of the clival line in the midportion of the FO. Regarding V3, the position of the electrode 5 mm beyond the clivus piercing the lateral portion of the FO targeted the V3 retrogasserian fibers in 100% of cases, compared with 0% if the tip was positioned 5 mm anterior to the clival line in

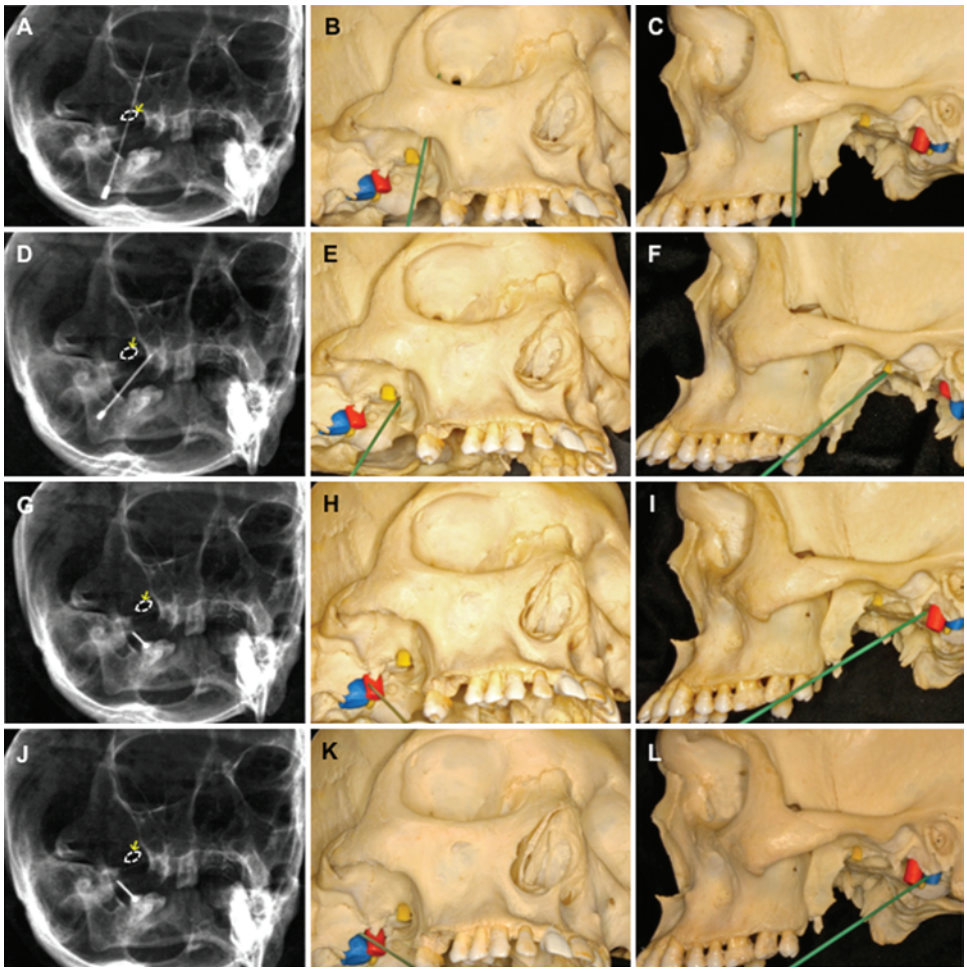

Fig. 9. Examples of incorrect placement of the needle in a 40°/45° inferior transfacial–20° oblique radiographic view *(left column)*, with corresponding anatomical *(center column)* and lateral views *(right column)*. The *white dashed ellipse* and *arrow* indicate the FO on the radiograph, and the yellow molding material indicates V3 in the FO in dry skulls. **A–C:** Needle in the orbit; note that on the radiograph, the FO, although posterior, is superimposed to this trajectory. **D–F:** Needle in the foramen lacerum; a lateral view (F) would not identify this misplacement. **G–I:** Needle injuring the carotid artery in the carotid foramen. **J–L:** Needle injuring the internal jugular vein, close to the jugular foramen.

the lateral view. In the last case, the electrode was located in the gasserian ganglion. Even with optimal trajectories, V1 continues to be the least selectively targeted (73.3%), followed by V2 (84.6%), and V3 (100%).

There is an angulation of the petrous bone in relation to the clivus and its projection in the lateral radiographic view (the clival line). The medial point of the trigeminal impression is closer to the clival line than the lateral point. With a correct trajectory, the more lateral the puncture is in the FO, the deeper the electrode can be inserted in relation to the clival line without passing the petrous ridge. Surprisingly, at a distance 5 mm anterior to the clival line in a lateral radiographic view, the electrode tip was most often found in the gasserian ganglion, so the lesion could be performed selectively in some cases, although it could be suboptimal.

An important limitation of the study is the absence of functional information as it is based on purely anatomical data that must be clinically confirmed in the future. As stated before, the position of the electrode tip that most efficiently reached the retrogasserian portion of the FO was 5 mm beyond the clival line for V1, V2, and V3. However, proceeding more than 2 mm away from the clival line when puncturing the medial portion of the FO or more than 4 mm when piercing the lateral portion could place the electrode tip beyond the petrous ridge in certain patients. These are the inferior safe limits that we found, but the average distance to the petrous ridge obtained in the specimens was greater (4.46 and 6.33 mm medially and laterally, respectively). Being aware of this anatomy, and with the functional information provided during the procedure, the surgeon must decide and individualize the depth of the insertion in each case.

Glycerol Rhizotomy. With glycerol rhizotomy, the insertion of the needle has to reach the trigeminal cistern. The safest and most efficient puncture is in the center of the middle third of the FO. The needle is advanced 1–2 mm incrementally until CSF is obtained, and then the procedure is stopped and glycerol is injected.[56] The needle should not advance away from the clival line, but rather remain in the trigeminal cistern in the Meckel

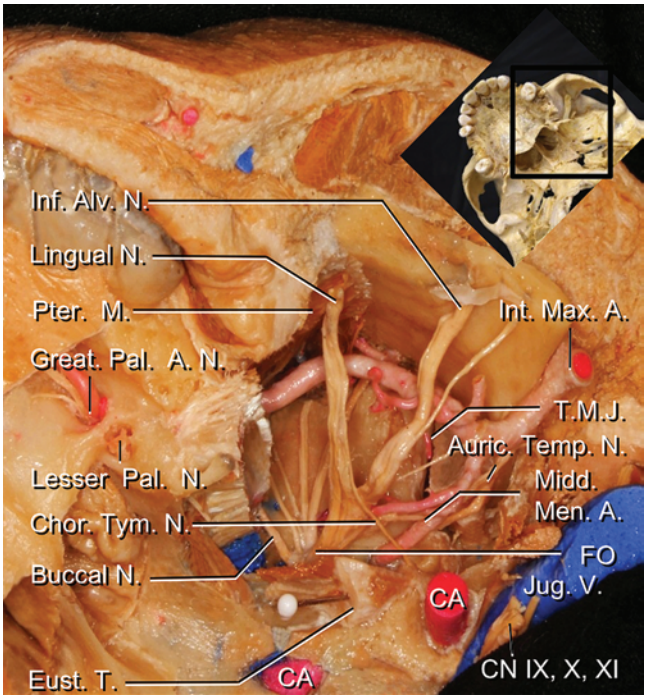

Fig. 10. Inferior view of the skull base and anatomical structures surrounding the third division of the TN that can be potentially injured with an incorrect puncture. Auric. Temp. N. = auriculotemporal nerve; CA = carotid artery; Chor. Tym. N. = chorda tympani nerve; CN = cranial nerve; Eust. T. = eustachian tube; Great. Pal. A. N. = greater palatine artery and nerve; Inf. Alv. N. = inferior alveolar nerve; Int. Max. A. = internal maxillary artery; Jug. V. = jugular vein; Lesser Pal. N. = lesser palatine nerve; Midd. Men. A. = middle meningeal artery; Pter. M. = pterygoid muscle; T.M.J. = temporomandibular joint.

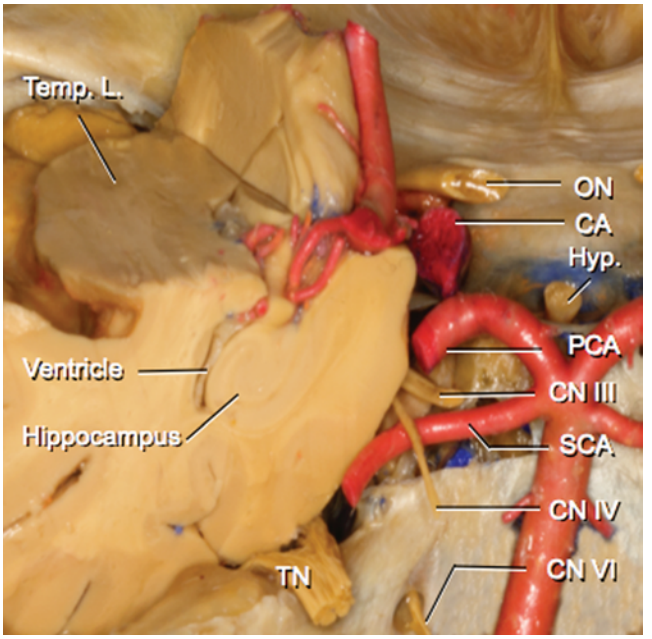

Fig. 11. Relationships of the temporal lobe and mesial structures with the TN, carotid artery (CA), and third and fourth cranial nerves (CN). After piercing the dura mater with the needle, the FO electrodes are positioned in the ambient cistern in contact with the mesial temporal structures. Hyp. = hypophyseal gland; ON = optic nerve; PCA = posterior cerebral artery; SCA = superior cerebellar artery; Temp. L. = temporal lobe.

cave. The distance from the FO to the common root of the TN over the petrous bone is 16 mm. Variations in the quantity of glycerol and head position of the patient have been used to obtain selective lesions of the TN. Because metrizamide is heavier than glycerol, if a small amount of it is left in the bottom of the cistern, it may protect V3 fibers in cases of V2 or V1 neuralgias.[15]

Percutaneous Balloon Microcompression. For percutaneous balloon microcompression, the needle is inserted in the FO, and the catheter is advanced.[30] The same anatomical principles as in radiofrequency ablation for selective puncture of the FO can be applied to the catheter position.

Foramen Ovale Electrode in Epilepsy. The trajectory to insert an FO electrode in epilepsy is not different from the FO puncture for trigeminal neuralgia,[40,50–54] apart from the need to pierce the dura mater to allow the electrode to be inserted adjacent to the mesial part of the temporal lobe in the ambient cistern. This insertion can be achieved by advancing the needle far enough to go through the dura mater (Fig. 11).

Conclusions

Knowledge of the anatomical and radiological landmarks of the percutaneous route to the FO is of essential importance to improve the technique and selectivity of the lesion, and to avoid complications. Our data suggest that better radiographic visualization of the FO can improve lesioning accuracy depending on the part of the FO to be punctured. The angles and safety distances obtained may help the neurosurgeon to minimize complications during FO puncture and TN lesioning. These results must be confirmed clinically in the future.

Disclosure

The Spanish Society of Neurosurgery partially supported this project through a grant given to Dr. Peris-Celda in 2010.

Author contributions to the study and manuscript preparation include the following. Conception and design: Peris-Celda, Mericle, Ulm. Acquisition of data: Peris-Celda, Graziano, Russo, Mericle. Analysis and interpretation of data: Peris-Celda, Mericle, Ulm. Drafting the article: Peris-Celda, Ulm. Critically revising the article: all authors. Reviewed submitted version of manuscript: all authors. Approved the final version of the manuscript on behalf of all authors: Peris-Celda. Administrative/technical/material support: Ulm. Study supervision: Ulm.

Acknowledgment

The authors are deeply grateful to Prof. Martinez-Soriano, University of Valencia, for providing some of the dry skulls used in this study.

References

1. Apfelbaum RI: Technical considerations for facilitation of selective percutaneous radiofrequency neurolysis of the trigeminal nerve. **Neurosurgery 3:**396–399, 1978

2. Barakos JA, Dillon WP: Lesions of the foramen ovale: CT-guided fine-needle aspiration. **Radiology 182:**573–575, 1992
3. Barker FG II, Jannetta PJ, Bissonette DJ, Larkins MV, Jho HD: The long-term outcome of microvascular decompression for trigeminal neuralgia. **N Engl J Med 334:**1077–1083, 1996
4. Berk C, Honey CR: Percutaneous biopsy through the foramen ovale: a case report. **Stereotact Funct Neurosurg 78:**49–52, 2002
5. Egan RA, Pless M, Shults WT: Monocular blindness as a complication of trigeminal radiofrequency rhizotomy. **Am J Ophthalmol 131:**237–240, 2001
6. Emmons WF, Rhoton AL Jr: Functional subdivision of the trigeminal sensory root. **Surg Forum 19:**440–441, 1968
7. Emmons WF, Rhoton AL Jr: Subdivision of the trigeminal sensory root. Experimental study in the monkey. **J Neurosurg 35:**585–591, 1971
8. Feiler V, Godel V, Lazar M: Sudden blindness after thermocoagulation of the trigeminal ganglion. **Ann Ophthalmol 22:**339–340, 1990
9. Gerber AM: Improved visualization of the foramen ovale for percutaneous approaches to the gasserian ganglion. Technical note. **J Neurosurg 80:**156–159, 1994
10. Gökalp HZ, Kanpolat Y, Tümer B: Carotid-cavernous fistula following percutaneous trigeminal ganglion approach. **Clin Neurol Neurosurg 82:**269–272, 1980
11. Gomori JM, Rappaport ZH: Transovale trigeminal cistern puncture: modified fluoroscopically guided technique. **AJNR Am J Neuroradiol 6:**93–94, 1985
12. Grunert P, Glaser M, Kockro R, Boor S, Oertel J: An alternative projection for fluoroscopic-guided needle insertion in the foramen ovale: technical note. **Acta Neurochir (Wien) 152:** 1785–1792, 2010
13. Gudmundsson K, Rhoton AL Jr, Rushton JG: Detailed anatomy of the intracranial portion of the trigeminal nerve. **J Neurosurg 35:**592–600, 1971
14. Gusmão S, Oliveira M, Tazinaffo U, Honey CR: Percutaneous trigeminal nerve radiofrequency rhizotomy guided by computerized tomography fluoroscopy. Technical note. **J Neurosurg 99:**785–786, 2003
15. Håkanson S: Trigeminal neuralgia treated by the injection of glycerol into the trigeminal cistern. **Neurosurgery 9:**638–646, 1981
16. Harris FS, Rhoton AL: Anatomy of the cavernous sinus. A microsurgical study. **J Neurosurg 45:**169–180, 1976
17. Harris W: An analysis of 1433 cases of paroxysmal trigeminal neuralgia (trigeminal-tic) and the end-results of gasserian alcohol injection. **Brain 63:**209–224, 1940
18. Härtel F: Die Behandlung der Trigeminusneuralgie mit intrakranieilen Alkoholeinspritzungen. **Deutsche Zeitschrift für Chirurgie 126:**429–552, 1914
19. Henderson WR: The anatomy of the gasserian ganglion and the distribution of pain in relation to injections and operations for trigeminal neuralgia. **Ann R Coll Surg Engl 37:**346–373, 1965
20. Horiguchi J, Ishifuro M, Fukuda H, Akiyama Y, Ito K: Multiplanar reformat and volume rendering of a multidetector CT scan for path planning a fluoroscopic procedure on Gasserian ganglion block—a preliminary report. **Eur J Radiol 53:**189–191, 2005
21. Kanpolat Y, Savas A, Bekar A, Berk C: Percutaneous controlled radiofrequency trigeminal rhizotomy for the treatment of idiopathic trigeminal neuralgia: 25-year experience with 1,600 patients. **Neurosurgery 48:**524–534, 2001
22. Kaplan M, Erol FS, Ozveren MF, Topsakal C, Sam B, Tekdemir I: Review of complications due to foramen ovale puncture. **J Clin Neurosci 14:**563–568, 2007
23. Kehrli P, Maillot C, Wolff MJ: Anatomy and embryology of the trigeminal nerve and its branches in the parasellar area. **Neurol Res 19:**57–65, 1997
24. Kuether TA, O'Neill OR, Nesbit GM, Barnwell SL: Direct carotid cavernous fistula after trigeminal balloon microcompression gangliolysis: case report. **Neurosurgery 39:**853–856, 1996
25. Lesley WS: Endosurgical repair of an iatrogenic facial arteriovenous fistula due to percutaneous trigeminal balloon rhizotomy. **J Neurosurg Sci 51:**177–180, 2007
26. Lobato RD, Rivas JJ, Sarabia R, Lamas E: Percutaneous microcompression of the gasserian ganglion for trigeminal neuralgia. **J Neurosurg 72:**546–553, 1990
27. Lopez BC, Hamlyn PJ, Zakrzewska JM: Systematic review of ablative neurosurgical techniques for the treatment of trigeminal neuralgia. **Neurosurgery 54:**973–983, 2004
28. McCann CF: Technique for needle biopsy in the foramen ovale region. **J Oral Surg 34:**463, 1976
29. Menzel J, Piotrowski W, Penzholz H: Long-term results of Gasserian ganglion electrocoagulation. **J Neurosurg 42:**140–143, 1975
30. Mullan S, Lichtor T: Percutaneous microcompression of the trigeminal ganglion for trigeminal neuralgia. **J Neurosurg 59:**1007–1012, 1983
31. Nathan H, Ouaknine G, Kosary IZ: The abducens nerve. Anatomical variations in its course. **J Neurosurg 41:**561–566, 1974
32. Nugent GR: Trigeminal neuralgia: treatment by percutaneous electrocoagulation, in Wilkins RH, Rengachary SS (eds): **Neurosurgery, ed 2.** New York: McGraw-Hill, 1996, Vol 3, pp 3945–3951
33. Onofrio BM: Radiofrequency percutaneous Gasserian ganglion lesions. Results in 140 patients with trigeminal pain. **J Neurosurg 42:**132–139, 1975
34. Ozveren MF, Sam B, Akdemir I, Alkan A, Tekdemir I, Deda H: Duplication of the abducens nerve at the petroclival region: an anatomic study. **Neurosurgery 52:**645–652, 2003
35. Ozveren MF, Uchida K, Erol FS, Tiftikci MT, Cobanoglu B, Kawase T: Isolated abducens nerve paresis associated with incomplete Horner's syndrome caused by petrous apex fracture—case report and anatomical study. **Neurol Med Chir (Tokyo) 41:**494–498, 2001
36. Parkinson D: Surgical anatomy of the lateral sellar compartment (cavernous sinus). **Clin Neurosurg 36:**219–239, 1990
37. Peters G, Nurmikko TJ: Peripheral and gasserian ganglion-level procedures for the treatment of trigeminal neuralgia. **Clin J Pain 18:**28–34, 2002
38. Rhoton AL Jr: Microsurgical neurovascular decompression for trigeminal neuralgia and hemifacial spasm. **J Fla Med Assoc 65:**425–428, 1978
39. Sekhar LN, Heros RC, Kerber CW: Carotid-cavernous fistula following percutaneous retrogasserian procedures. Report of two cases. **J Neurosurg 51:**700–706, 1979
40. Siegfried J, Wieser HG, Stodieck SR: Foramen ovale electrodes: a new technique enabling presurgical evaluation of patients with mesiobasal temporal lobe seizures. **Appl Neurophysiol 48:**408–417, 1985
41. Sweet WH, Wepsic JG: Controlled thermocoagulation of trigeminal ganglion and rootlets for differential destruction of pain fibers. 1. Trigeminal neuralgia. **J Neurosurg 40:**143–156, 1974
42. Tatli M, Satici O, Kanpolat Y, Sindou M: Various surgical modalities for trigeminal neuralgia: literature study of respective long-term outcomes. **Acta Neurochir (Wien) 150:**243–255, 2008
43. Tatli M, Sindou M: Anatomoradiological landmarks for accuracy of radiofrequency thermorhizotomy in the treatment of trigeminal neuralgia. **Neurosurgery 63 (1 Suppl 1):**ONS129–ONS138, 2008
44. Tator CH, Rowed DW: Fluoroscopy of foramen ovale as an aid to thermocoagulation of the Gasserian ganglion; technical note. **J Neurosurg 44:**254–257, 1976
45. Tew JM Jr, Keller JT: The treatment of trigeminal neuralgia by percutaneous radiofrequency technique. **Clin Neurosurg 24:**557–578, 1977

46. Tew JM Jr, Keller JT, Williams DS: Application of stereotactic principles to the treatment of trigeminal neuralgia. **Appl Neurophysiol 41:**146–156, 1978
47. Tew JM Jr, Lockwood P, Mayfield FH: Treatment of trigeminal neuralgia in the aged by a simplified surgical approach (percutaneous electrocoagulation). **J Am Geriatr Soc 23:**426–430, 1975
48. Tobler WD, Tew JM Jr, Cosman E, Keller JT, Quallen B: Improved outcome in the treatment of trigeminal neuralgia by percutaneous stereotactic rhizotomy with a new, curved tip electrode. **Neurosurgery 12:**313–317, 1983
49. Whisler WW, Hill BJ: A simplified technique for injection of the Gasserian ganglion, using the fluoroscope for localization. **Neurochirurgia (Stuttg) 15:**167–172, 1972
50. Wieser HG, Elger CE, Stodieck SR: The 'foramen ovale electrode': a new recording method for the preoperative evaluation of patients suffering from mesio-basal temporal lobe epilepsy. **Electroencephalogr Clin Neurophysiol 61:**314–322, 1985
51. Wieser HG, Hajek M: Foramen ovale and peg electrodes. **Acta Neurol Scand Suppl 152:**33–35, 1994
52. Wieser HG, Schwarz U: Topography of foramen ovale electrodes by 3D image reconstruction. **Clin Neurophysiol 112:** 2053–2056, 2001
53. Wieser HG, Siegel AM: Analysis of foramen ovale electrode-recorded seizures and correlation with outcome following amygdalohippocampectomy. **Epilepsia 32:**838–850, 1991
54. Wieser HG, Zumsteg D: A model for foramen ovale puncture training: technical note. **Acta Neurochir (Wien) 148:**1127–1129, 2006
55. Yang Y, Shao Y, Wang H, Liu Y, Zhu S, Wu C: Neuronavigation-assisted percutaneous radiofrequency thermocoagulation therapy in trigeminal neuralgia. **Clin J Pain 23:**159–164, 2007
56. Young RF: Percutaneous trigeminal glycerol rhizotomy, in Rengachary SS, Wilkins RH (eds): **Neurosurgical Operative Atlas.** Chicago: AANS, 1991, Vol 1, pp 117–123

Manuscript submitted May 23, 2012.
Accepted January 30, 2013.
Partial contents of this article were presented as an awarded poster in the pain section of the AANS Meeting in Denver, Colorado, in April 2011; as an oral presentation at the Spanish Congress of Neurosurgery in Madrid, Spain, in May 2011; and as a poster at the International Symposium on Microneurosurgical Anatomy Congress in Istanbul, Turkey, in November 2010.
Please include this information when citing this paper: published online April 19, 2013; DOI: 10.3171/2013.1.JNS12743.
Current affiliation for Drs. Mericle and Ulm: HW Neurological Institute, Nashville, Tennessee.
Current affiliation for Dr. Peris-Celda: Department of Neurosurgery, University of Florida, Gainesville, Florida.
Address correspondence to: Maria Peris-Celda, M.D., Ph.D., Department of Neurosurgery, School of Medicine, LSU Health Sciences Center, 2020 Gravier Street, 7th Floor, New Orleans, Louisiana 70112. email: mperiscelda@gmail.com.